De novo design, synthesis and spectroscopic characterization of ,2–diaminobenzene, dichloro glycyl glycinate tin(IV) and zirconium(IV) complexes: *In vitro* DNA binding, DNA cleavage pathway and molecular docking investigations

Waddhaah M. Alasbah*, and Manal Shamsi

*Department of Chemistry, Taiz University, Taiz, Yemen.

* Corresponding author: Tel.: +967777439393
E–mail address: wadahm2007@yahoo.com (WM Alasbahy)

Abstract— De novo design and synthesis of complexes 1,2–diaminobenzene,dichloro glycyl glycinate tin(IV) and zirconium(IV), **1** and **2** as molecular drug entities were carried out. The structure elucidation of **1** and **2** wasdone by analytical techniques and spectroscopic methods viz. IR, UV–vis, ^{1}H, ^{13}C, ^{119}Sn NMR, ESI–Mass techniques. *In vitro* DNA binding studies of **1** and **2** by various biophysical techniques *viz* electronic absorption, emission spectroscopy and circular dichroism measurements was carried out to evaluate their potential to act as chemotherapeutic candidates; furthermore, cleavage studies with pBR322plasmid DNA and computer–aided molecular docking studies were also done to study the mechanistic pathway and mode of binding at the molecular level.The observed results revealed that the complex **1** exhibited greater DNA binding propensity in contrast to the complex **2** primarily via electrostatic binding mode. The pBR322 DNA cleavage studies of both the complexes revealed the hydrolytic cleavage mechanismand DNA minor groove binding, which was ascertained by molecular docking studies of the drug candidate.

Keywords: Sn(IV) and Zr(IV) glycyl glycine complexes; DNA binding profile; pBR322cleavage, molecular docking

1 INTRODUCTION

Metal–based antitumor chemotherapeutic drugs have gained considerable interest after the serendipitous discovery of cisplatin, an archetypical metal complex in clinical use for treating solid malignancies [1,2]. Although the platinum drugs have witnessed spectacular success, nevertheless, the challenges of platinum drugs such as systemic toxicity, resistance and large number of phenotypes of cancers derived from multiple etiologies have motivated researchers to focus on other non platinum drugs. A substantial investigation of other metals as antitumor chemotherapeutic agents which includes (transition metal ions Ti, Fe ,Co ,Cu and Zn ; Zr, Ru, Rh ,Pd, Ag, Au and non– transition metal ions , Sn and R_2SnX_2 has been undertaken to overcome the problems of toxic side effects and resistance (Blower and Annu, 2004; van Rijt and Sadler, 2009). Tin (IV) complexes were proven as outstanding class of novel antitumor and antiproliferative agents; much of the earlier work has been carried out by Crowe *et al* and Gielen [3–5] which has been published and also patented. Tin(IV) and Organotin compounds are involved in cancer treatment via different mechanisms at the molecular level and most of the tin complexes are DNA targeted . The phosphate group of DNA sugar backbones usually acts as an anchoring site and nitrogen of DNA base binding is extremely effective, this often resulting in the stabilization of the tin center as an octahedral species.Literature revealed that tin–based complexes exhibit pronounced cytotoxicity against human cell lines [6] viz., Hela cells, MCF–7 cells and human neuroblastoma cell line SY5Y [7] and further, it has also been demonstrated that these complexes induce apoptosis via mitochondrial genemediated pathway. Among the non–platinum chemotherapeutics, tin(IV) and by electronic analogy, zirconium(IV) complexes with amino acid scaffold and non–leaving diammine ligands are interesting as they could exhibit different mechanism of action than platinum complexes and relatively fewer toxic effects. Moreover, Zr(IV) is expected to act exclusively as a strong Lewis acid and Zr(IV) complexes catalyze the hydrolysis of phosphodiester and dinucleotides under weakly acidic conditions. Zirconium complexes reported in the literature (Zirconocene–diacido complexes) exhibit wide spectrum of antitumor activity against murine and human tumors with reduced toxicity in comparison with cisplatin [8]. Among them, synthetic agents capable of hydrolytically cleaving nucleic acids are extremely important and have been attracting increasing attention in view of their wide applications. On the one hand, artificial hydrolytic catalysts may be employed as biomimetic systems in elucidating the mechanisms of the corresponding restriction enzymes and nucleases, and they could also be used as conformational probes in the determination of DNA structure, as customized DNA restriction agents in molecular biology, and as antibiotic and chemotherapeutic drugs.

It is well known that peptides and proteins are the naturally occurring multifunctional ligands and forms an excellent

coordination platform because they contain a variety of potential donor centers such as N–terminal nitrogen atom (usually a primary —NH_2), carbonyl oxygen and the C–terminal carboxylate group of the peptide bond [9]. The metallopeptides are considered unique among metal–based nucleic acid–binding agents due to their ability to recognize DNA ornucleotides. The nature of the peptide affects both the DNA binding affinity and the cross linking efficiency of metallopeptides and have been widely used as synthetic hydrolyses and chemical nucleases [10,11]. Among the numerous metal complexes investigated, those containing amino acids and/ or peptide ligands provide models of protein–DNA and metallopeptide–derived antitumor agent–DNA interaction [12]. Recently, a science daily has reported that peptides could target the protein–protein interface of a key enzyme in DNA synthesis crucial for cancer growth [13]. Therefore, metal–based peptide scaffolds could provide an excellent delivery system into the specific tumor target sites and could be less toxic to normal tissues. Previous studies reveals that interaction of peptides with organotin moieties is quite interesting since peptides can be very effective ligands and furthermore it has been demonstrated that these organotindipeptide complexes shows modest activity against P388 lymphocytic leukemia cells.Moreover it has been reported by R. Krameret al thatconjugates of peptide nucleic acids and Zr(IV) complexes efficiently hydrolyze complementary single–stranded DNA in a sequence selective fashion [14,15]. Herein we report the synthesis and characterization of mixed ligand tin(IV) and zirconium(IV) complexes derived from 1,2–diaminobenzene and glycyl glycine ligand scaffold as potential chemo–therapeutic drug candidates. *In vitro* binding studies of these complexes with CT–DNA and nucleotide were explored by absorption and emission titration methods to elucidate their mode of binding and pharmacological potential. The pBR322 DNA cleavage studies of both the complexes revealed the hydrolytic cleavage mechanismand DNA minor groove binding. Furthermore, computer–aided molecular docking studies were carried out to visualize the binding mode of the drug candidate (minor groove binding) at the molecular level.

2 Procedure for Paper Submission

2.1 Reagents and materials

All reagents were commercially available and used as supplied without further purification for all syntheses and experiments. Glycyl glycine (Glygly), o–phenylenediamine (OPD), Tris(hydroxymethyl)aminomethane or Tris buffer, agarose gel, ascorbic acid, sodium azide (NaN_3), DMSO, superoxide dismutase (SOD), methyl green, DAPI, mercaptopropionic acid (MPA) (Sigma–Aldrich), $SnCl_4.5H_2O$ and $ZrCl_4$ (Fisher Scientific), 6X loading dye (Fermental Life Science), Human DNA topoisomerase I (Calbiochem) and Supercoiled pBR322 plasmid DNA (Genei) were utilized as received. Disodium salt of CT DNA purchased from Sigma Chem. Co. and was stored at 4 °C. DNA–melting experiments were carried out by monitoring the absorbance of CT DNA (1×10^{-4} M) at 260 nm with varying temperature in the absence and presence of complexes **1** and **2,** in a 1:1 ratio of DNA to complex with a ramp rate of $0.1^{\circ}C\ min^{-1}$ in Tris buffer (pH 7.2) using a Peltier system attached to the UV–Vis spectrophotometer.

.

2.2 Methods and Instrumentation

Carbon, hydrogen and nitrogen contents were determined using CHNSO Elemental Analyzer ElementarVario EL IIImodel. Molar conductance was performed at room temperature on a Digisun electronic conductivity bridge. Fourier–transform IR (FTIR) spectra were recorded on an Interspec 2020 FTIR spectrometer. Electronic spectra were recorded on UV–vis 1700 PharmaSpec UV–vis spectrophotometer (Shimadzu). Data were reported in λmax/nm. The 1H and 13C NMR spectra were obtained on a Bruker DRX–400 spectrometer operating at room temperature. Solutions of CT DNA in buffer gave a ratio of absorbance at 260 nm and 280 nm of ca. 1.9 indicating that DNA was free from protein. CD spectra were measured on Jasco J–815–CD spectropolarimeter at room temperature using a 1 cm quartz cuvette. Cleavage experiments were performed with the help of Axygen electrophoresis supported by a Genei power supply with a potential range of 50–500 V, visualized and photographed by Vilber INFINITY gel documentation system.

2.3.DNA–binding and cleavage experiments

DNA binding experiments include absorption spectral traces, emission spectroscopy and circular dichroism conformed to the standard methods and practices previously adopted by our laboratory [16]. While measuring the absorption spectra an equal amount of DNA was added to the compound solution and the reference solution to eliminate the absorbance of the CT DNA itself, and the CD contribution by the CT DNA and Tris buffer was subtracted through base line correction.

The cleavage experiments of supercoiled pBR322 DNA (300 ng) by complex 1 and 2 (10–30 μM) in Tris–HCl/NaCl (5:50 mM) buffer at pH 7.2 was carried out using agarose gel electrophoresis. The samples were incubated for 45 min at 310 K. A loading buffer containing 25% bromophenol blue, 0.25% xylene cyanol, 30% glycerol was added and electrophoresis was carried out at 50 V for 1 h in Tris–HCl buffer using 1% agarose gel containing 1.0 mg/ml ethidium bromide. The DNA cleavage with added reductant was monitored as in case of cleavage experiment without added reductant using agarose gel electrophoresis.

2.4. Molecular docking

The rigid molecular docking studies were performed by using HEX 6.1 software [16], which is an interactive molecular graphics program to understand the drug–DNA interactions. The Structure of the complexes was sketched by CHEMSKETCH (http://www.acdlabs.com) and converted to pdb format from mol format by OPENBABEL (http://www.vcclab.org/lab/babel/). The structure of the B–DNA dodecamer (CGCGAATTCGCG)2 (PDB ID:1BNA) and human–DNA–Topo I complex (PDB ID: 1SC7) were downloaded from the protein data bank (http://www.rcsb.org./pdb). All calculations were carried out on an Intel Pentium 4, 2.4 GHz based machine running MS Windows XP SP2 as operating system. Visualization of the

docked pose has been done by using CHIMERA (http://www.cgl.ucsf.edu/chimera/) molecular graphics program.

2.5 Synthesis

2.5.1 Synthesis of $C_{10}H_{22}N_4O_7Cl_2Sn$ (1)

To a stirred methanolic solution (15 ml) of glycyl glycine (0.130 g, 1mmol) was added a methanolic solution (15 ml) of $SnCl_4.5H_2O$ (0.343 g, 1 mmol). The solution was stirred for 24 h at room temperature. The completion of the reaction was monitored with the help of TLC. A solution of o–phenylenediamine (0.108 g. 1 mmol) in methanol was added slowly to the reaction mixture. The reaction mixture was refluxed at 65 °C for 8 h, which yielded pale reddish orange colored precipitate. It was filtered, washed with cold MeOH and dried in vacuo over anhydrous $CaCl_2$. Yield = 70%. M.P. = 120 ± 2°C. Anal. Calc. for $C_{10}H_{22}N_4O_7Cl_2Sn$, (%) C, 24.03 H, 4.44; N, 11.21, Found: C, 22.19; H, 4.08; N, 10.31. IR (KBr, cm^{-1}): 3277 ν(NH_2); 1746: ν(COO); 2825 ν(CH); 1583 ν(C=C); 1678 ν_{as}(COO); 1492 ν_s(COO); 1349 ν(C–N); 754 (Ar); 583 ν(Sn–O); 440 ν(Sn–N).Molar Conductance, Λ_M (1×10^{-3} M, H_2O): 22 $\Omega^{-1}cm^2\ mol^{-1}$ (non–electrolyte). ^{1}H NMR (400 MHz, D_2O, δ): 3.63 (NCH_2, peptide), 3.98 (–CH_2, peptide), 4.72 NH_2 (coordinated, OPD), 3.70 NH_2 (free OPD), 7.40–7.43 (protons of phenyl groups). ^{13}C NMR (100 MHz, D_2O, δ): 172.84 (O–C=O–NH_2); 167.34 (CH_2–C=O); 149.28 (ArC–NH_2, coordinated OPD); 130.16 (ArC–NH_2, free OPD); 113.65–127.06 (ArC); 40.93 (NH_2–CH, peptide); 35.37 (–CH_2, peptide). ^{119}Sn NMR (149.12 MHz, DMSO, δ): –611.49. Uv–vis absorption: λ_{max} (H_2O, 10^{-3} M), nm ($\varepsilon/10^3\ M^{-1}\ cm^{-1}$) 230 (2.11), 278 (1.24) and 457 (0.80). ESI–MS (m/z): [$C_{10}H_{22}N_4O_7\ Cl_2Sn$] ; 499.2.

2.5.2 Synthesis of $C_{10}H_{18}N_4O_5ZrCl_2$ (2)

This complex was prepared in a manner analogous to that of complex **1**, using $ZrCl_4$ (0.233 g, 1 mmol) in place of $SnCl_4.5H_2O$ (0.343 g, 1 mmol), resulting the pale orange colored product. It was filtered, washed with cold MeOH and dried in vacuo over anhydrous $CaCl_2$. Yield = 59%. M.P. = 145 ± 2°C. Anal. Calc. for$C_{10}H_{18}N_4O_5ZrCl_2$ (%) C, 27.5; H, 4.16; N, 12.8, Found: C, 25.05; H, 4.56; N, 11.38.IR (KBr, cm^{-1}):3408 ν(NH_2); 2928 ν(CH); 1734: ν(COO); 1563 ν(C=C); 1678 ν_{as}(COO); 1452 ν_s(COO); 1317 ν(C–N); 758 (Ar); 527 ν(Zr–O); 452 ν(Zr–N). Molar Conductance, Λ_M (1×10^{-3} M, H_2O): 19 $\Omega^{-1}cm^2\ mol^{-1}$ (non–electrolyte). ^{1}H NMR (400 MHz, D_2O, δ): 3.54 (NCH_2, peptide); 3.86 (–CH_2, peptide); 4.72 NH_2 (coordinated, OPD), 3.84 NH_2 (free OPD), 6.84–6.91 (protons of phenyl groups). ^{13}C NMR (100 MHz, D_2O, δ): 170.78 (O–C=O–NH_2); 166.16 (CH_2–C=O); 117.2–132.57 (ArC); 38.7 (NH_2–CH, peptide); 39.79 (–CH_2, peptide). Uv–vis absorption: λ_{max} (D_2O, 10^{-3} M), nm ($\varepsilon/10^3\ M^{-1}\ cm^{-1}$): 230 (1.23), 283 (0.66) and 451 (0.36).ESI–MS (m/z): [$C_{10}H_{18}N_4O_5ZrCl_2$] 436.2.

3 Results and Discussion

3.1 Synthesis and characterization

All the complexes are readily soluble in H_2O solvent. In complexes **1** and **2**, the coordination geometry of central metal atoms was found to be octahedral environment (Scheme 1 and 2), which was proposed on the basis of elemental analytical data and spectroscopic studies, IR, UV–vis, ESI–MS ^{1}H, ^{13}CNMR (^{119}Sn NMR in case of **1**). These results are in agreement with the proposed 1:1:1 stoichiometry between the metal ion and ligands. The *in vitro* binding studies of **1** and **2** with CT DNA were carried out by using absorption, emission titrations and circular dichroic studies. Furthermore, the cleavage studies of **1** and **2** with pBR322 plasmid DNA and molecular docking with DNA by computational methods were carried out.

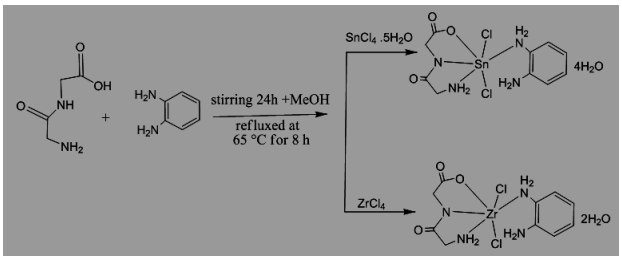

Scheme 1. The synthetic of complexes **1** and **2**.

3.1.1 Infrared spectra

The IR spectra of complexes **1** and **2** agree with the corresponding formulae and the proposed structure (Scheme 1). The bands around 1678 and 1452–1492 cm^{-1}observed in the free amino acid corresponding to the anti–symmetric and symmetric COO^- stretching vibrations were shifted inthe complexes suggesting the coordination of carboxylate group of the amino acid to the metal ions through deprotonation [17]. The bands around 1531 and 1269 cm^{-1} observed in the free dipeptide attributed to amide II and III bands [due to δ(NH) + ν(C–N) in the compound containing neutral secondary peptide groups were replaced by a new absorption bands at 1349 and 1317 cm^{-1}, respectively in complexes **1** and **2**.This is characteristic feature for a deprotonated secondary peptide complex, since on removal of peptide proton the band becomes a pure C–N stretch [18].

The $\Delta\nu = [\nu_{as}(CO_2) - \nu_s(CO_2)]$ value was used to determine the nature of binding of carboxylate to transition metal ion. In general, the difference in Δν between asymmetric $\nu_{as}(CO_2)$ and symmetric $\nu_s(CO_2)$ absorption frequencies below 200 cm^{-1} suggested the bidentate carboxylate moiety, while greater than 200 cm^{-1} implicates the unidentate carboxylation. In all cases, the Δν values were above 235 cm^{-1} suggestive of coordination of the carboxylate group in a monodendate fashion [19,20]. The IR spectra of the complexes **1** and **2** exhibited a very broad band at ~3277–3408 cm^{-1} corresponding to the coordinated dipeptide of glycyl glycine and o–phenylenediamine, suggesting that the coordination of –NH_2 group of both dipeptide and o–phenylenediamine to the metal ions [21]. Furthermore, the medium intensity bands at ~440–452 and 527–583 cm^{-1} were attributed to stretching vibration of(Sn/Zr–N), (Sn/Zr–O), respectively [22].

3.1.2 Nuclear magnetic resonance spectra

The ^{1}H and ^{13}C NMR spectra of complexes **1** and **2** were recorded in DMSO–d6 solution and displayed signals for aliphatic and aromatic protons with chemical shift values in accordance with their proposed structure. In ^{1}H NMR spectrum of complex **1**, signals due to free carboxylic (COOH) and amide linkage (–NH–) groups as expected in the range 12.0–10.0, 12.55 and 11.81 ppm, respectively were absent, which commensurate with the fact that coordination to the metal center takes place of these functional groups *via* deprotonation [23,24]. Additionally, the ^{1}H spectra exhibited characteristic resonance signals at 3.63–3.54 and 3.98–3.86 ppm corresponding to the NCH_2 and CH_2 proton of the peptide, the aromatic proton of o–phenylenediamine appeared as a multiplet at 6.84–7.40 ppm [25,26]. The ^{13}C NMR spectra of complexes **1** and **2** were characterized by various resonances due to O–C=O, CH_2–C=O, ArC–NH_2, NH_2–CH and –CH_2 carbons at 172.84–170.78, 166.16, 40.93–38.7, 35.37–39.79 ppm, respectively of the coordinated dipeptide and o–phenylenediamine. Additionally, complexes **1** and **2** exhibited aromatic carbon signatures at 117–132 ppm. The ^{119}Sn chemical shift, $\delta(^{119}Sn)$ is sensitive to the chemical environment of the tin atom. The ^{119}Sn NMR of complex **1** displayed a single peak at −611 ppm indicating octahedral geometry of tin atom [27,28].

3.1.3 Mass spectroscopy

The formation of metal complexes and the speciation of various ionic forms in H_2O solution were studied with ESI–MS. The spectra of the complexes **1** and **2** displayed prominent peaks corresponding to the molecular ion fragment at 499.2 and 436.2, respectively. Major peaks at m/z: 357.1 and 249.1 were observed for complex **1** corresponding to the fragments [$C_{10}H_{22}N_4O_7$ Cl_2 Sn –$4H_2O$ – 2Cl], and [$C_{10}H_{22}N_4O_7$ Cl_2 Sn –$4H_2O$ – 2Cl – OPD]. The complex **2** exhibited peaks at m/z: 329.1 and 221.1 ascribed to the fragments [$C_{10}H_{18}N_4O_5ZrCl_2$–$2H_2O$–2Cl] and [$C_{10}H_{18}N_4O_5ZrCl_2$–$2H_2O$ –2Cl– OPD], respectively.

3.1.4 Electronic spectra

The electronic absorption spectra of complexes **1** and **2** were obtained in the region 200– 1100 nm at room temperature. The electronic spectrum of free dipeptide displayed intense absorption bands at 220 nm due to an n → π* transition which was shifted to ~230 nm upon coordination with metal ions, and has been assigned to a N^{-}→(Sn/Zr) ligand to metal charge transfer (LMCT) transition (Dehand et al., 1979). A broad band at 278 nm was attributed to π → π* transitions of carboxylate group (COO^{-}) of dipeptide to the metal ion (charge transfer transition).

3.2 DNA binding studies

3.2.1 Electronic absorption titration

Electronic absorption spectrum is one of the most commonly used tools for the study of the development of the binding of DNA with metal complexes. The absorption spectra of complexes **1** and **2** in the absence and presence of CT–DNA at constant concentration of complexes are shown in Fig. 1(a, b). The complexes **1** and **2** exhibited intraligand absorption bands in the UV region at 230 and 278 nm, respectively. On addition of CT–DNA (increasing concentration [(0.066–0.333)×10^{-4} M] to complexes **1** and **2**, there is a sharp hyperchromism with a significant blue shift of~3–5 nmin the absorption bandattributed to the electrostatic binding mode and stabilization of the complex–DNA adduct [29,30]. Moreover, 'hyperchromic' effect reflects the corresponding changes of DNA in its conformation and structure after the complex–DNA interaction has taken place due to (i) external contact (surface binding) with the duplex through hydrogen bonding interactions between coordinated –NH_2 and oxygen atoms of the ligands with the edge of DNA bases which are accessible both in the major and minor grooves, (ii) coordinate covalent binding to N7/N3 of the base pairs of DNA due to the replacement of the labile water molecule. Also, the presence of aromatic moieties could facilitate partial intercalation by insertion of the complexes into the adjacent base pairs of DNA.

To evaluate the binding ability of the complexes **1** and **2** with CT– DNA, the intrinsic binding constants K_b of the complexes were determined from Wolfe–Shimer Eq. (1) by monitoring the changes in absorbance bands with increasing concentration of CT–DNA [31]:

$$\frac{[DNA]}{[\varepsilon_a - \varepsilon_f]} = \frac{[DNA]}{[\varepsilon_b - \varepsilon_f]} + \frac{1}{K_b[\varepsilon_b - \varepsilon_f]} \quad (1)$$

Where *[DNA]* represents the concentration of DNA, ε_a, ε_f and ε_b are the apparent extinction coefficient A_{obs}/[M], the extinction coefficient for free metal complex and the extinction coefficient for metal complex in the fully bound form, respectively. In the plots of $[DNA]/\varepsilon_a - \varepsilon_f$ versus *[DNA]*, K_b is given by the ratio of the slope to the intercept. The binding constant obtained for **1** and **2** were found to be 5.17×10^4 and 2.64×10^4 M^{-1}, respectively.The K_b values revealed that **1** exhibited greater propensity towards CT DNA than **2**, thereby shows stronger binding affinity.

To further investigate the selective recognition and validate the binding mode of the complexes **1** and **2** withCT–DNA via electrostatic binding, the interaction of complexes **1** and **2** was carried out with nucleotide 5′–GMP. The absorption spectra of complexes **1** and **2** in presence of 5′–GMP are shown in Fig. 2(a, b). On addition of 5′–GMP to the complexes **1** and **2**, there was a sharp increase ''hyperchromic'' effect in the absorption bands at ~278 nmwith no shift in absorbance. This observation supports the binding of metal (Sn/Zr) complexes *via* electrostatic interaction mode as observed in case of CT DNA. The intrinsic binding constant K_b values for **1**and **2** were found to be 3.4×10^4 and 1.77×$10^4$$M^{-1}$, respectively and the extent of binding of Sn(IV) **1** and Zr(IV) **2** was of the order **1**> **2**, respectively which revealed higher preference of Sn(IV) complex to the 5′–GMP as compared to Zr(IV) complex.

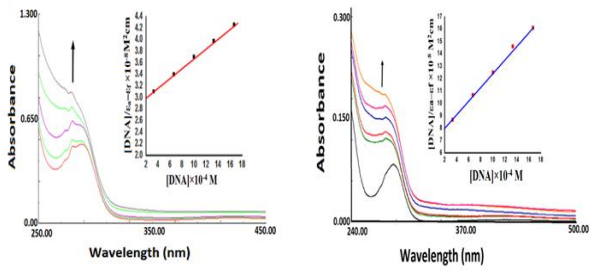

Fig. 1. Absorption spectral traces of complexes (a) **1,** (b) **2**in 5mM Tris HCl / 50 mM NaCl buffer at pH 7.2 upon addition of CT DNA. Inset: Plots of [DNA]/ $\varepsilon_a-\varepsilon_f$ (M^2cm)*vs* [DNA] for the titration of CT DNA with complexes (■), experimental data points; full lines, linear fitting of the data. [Complex] 1.00 × 10^{-4}M, [DNA] 0.066–0.333 × 10^{-4} M.

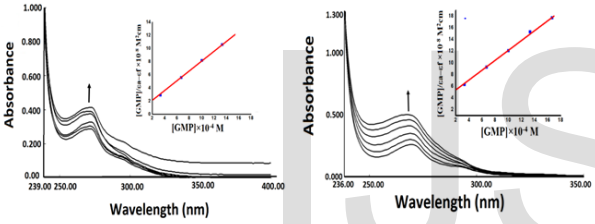

Fig. 2. Variation of UV–vis absorption for complexes (a) **1**, (b) **2** with increase in the concentration of 5′ GMP (0.067×10^{-4}– 0.33 ×10^{-4}M) in buffer (5mM Tris–HCl/50 mM NaCl, pH= 7.2) at room temperature. Inset: plot of [5′–GMP]/ (εa–εf) *vs* [5′–GMP] for the titration of 5′– GMP.

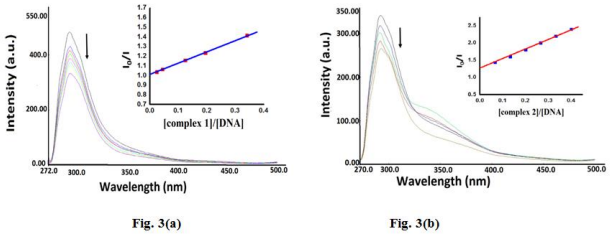

Fig. 3(a) Fig. 3(b)

Fig. 3. Emission spectra of EB bound to DNA in the absence and presence complexes (a) **1**, (b) **2** in 5 mM Tris–HCl/50 mM NaCl buffer. Arrows show the intensity changes upon increasing concentration of the complex. Inset: Plots of I_0/I*vsr* (= [complex]/ [DNA]). (■) experimental data points; full lines, linear fitting of the data.

3.2.2 Ethidium bromide displacement assay

In the absence of CT–DNA, no luminescence was observed for complexes **1** and **2** eitherin aqueous solution, in any organic solvent or in the presence of DNA. Hence, the binding of complexes **1** and **2** with CT–DNA cannot be directly predicted through the emission spectra. Therefore, interaction of the complexes **1** and **2** with CT–DNA was carried out by acompetitive binding experiment using ethidium bromide (EB) as a probe.EB (3,8–diamino–5–ethyl–6–phenylphenanthrium bromide), a phenanthridine fluorescence dye, is a typical probe for intercalation (Wilson et al., 1993) form soluble complexes with CT–DNA and emits intense fluorescence when intercalated into the base pairs of DNA [32]. The addition of the complexes to DNA pretreated with EB ([DNA]/[EB] =1) solution caused an appreciable reduction in fluorescence intensity due to replacement of EB by the complexes [33]. The complexes **1** and **2** showed decrease in the emission intensity of EB–DNA system Fig. 3(a, b), which indicated that the complexes **1** and **2** were bind to DNA *via* electrostatic interactions releasing EB molecules gradually from the EB–DNA system [34]. The quenching efficiency for each complex was evaluated by using Stern–Volmer equation:

$$I_0/I = 1 + K_{SV}.r \qquad (2)$$

Where I_0 and I represent the fluorescence intensities in the absence and presence of the complexes **1** and **2** respectively; r is the concentration ratio of the complex to DNA, and K_{SV} is used to evaluate the quenching efficiency and is obtained as the slope of I_0/I*vs*. r (=[complex]/[DNA]). The K_{SV} value for the complexes **1** and **2** were found to be 2.25 and 1.51, respectively, the maximum value obtained for complex **1** is in agreement with its highest K_b value, i.e. Complex **1** binds to CT–DNA very strongly, hence maximum quenching.

3.2.3 Circular dichroism

The circular dichroism pattern observed for CT–DNA provide further and definitive conformational of the DNA binding event with complexes **1** and **2**.The CD spectrum of CT–DNA exhibits a positive band at 278 nm (UV: λ_{max}, 260 nm) due to base stacking and a negative band at 240 nm due to the right–handed helicity of B–DNA form which are quite sensitive to the mode of DNA interactions with complexes. Groove binding and electrostatic interaction of the complexes with DNA are known to exhibit only marginal changes in the intensity of both negative band as well as the positive band of DNA. On the other hand, intercalators are known to enhance the intensities of both these bands [35]. The CD spectrum of DNA exhibited decrease in intensity of both positive and negative bands when the complexes **1** and **2** were incubated with CT DNA suggesting that the complexes could unwind the DNA helix and lead to loss of helicity. Incubation of B–DNA with complexes **1** and **2** induced marginal changes both in its positive and negative bands retaining the basic shape which suggested that the binding of the complexes retained B–conformational form of DNA [36] revealing the electrostatic binding mode and groove binding interactions consistent with the other DNA binding studies.

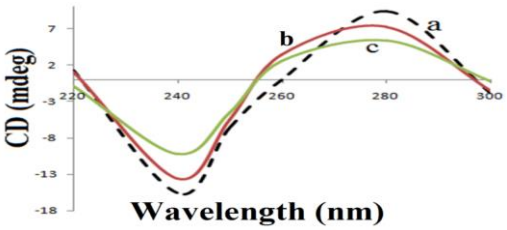

Fig. 4. CD spectra of (a) CT DNA alone, (b) in the presence of **1**, (c) in the presence of **2**. [Complexes] = 1×10^{-4} M, [DNA]= 1×10^{-4} M.

3.3 DNA cleavage assay

3.3.1 DNA cleavage without added reductant

In order to assess the chemical nuclease activity of complexes **1** and **2**, agarose gel electrophoresis was performed using pBR322 plasmid DNA as a substrate in a medium of 5 mM Tris–HCl/50 mM NaCl buffer, at pH 7.2 without addition of any reductant. When circular plasmid DNA was subjected to gel electrophoretic mobility assays, relatively fast migration was observed for the intact supercoiled Form (I). However, if scission of DNA occurs atone strand (nicking), the supercoiled DNA converted into a slowermoving open/nicked circular Form (II). If both strands cleaved, a linear Form (III) was generated [37]. A concentration dependent DNA cleavage by complexes **1** and **2** was first performed in which pBR322 DNA (300 ng) was incubated at 310 K for 45 min. As shown in Fig. 5, with the increase of concentration of **1** and **2**, DNA was converted from Form I (Supercoiled Form) to Form II (Nicked Circular Form) and then to Form III (Linear Form), which indicates that the complexes are capable of performing direct double strand scission of DNA.

3.3.2 In presence of activators

The mechanistic pathway of DNA cleavage mediated by complexes was investigated by gel electrophoresis in the presence of various activators viz., glutathione (GSH), ascorbic acid (Asc), hydrogen peroxide (H_2O_2) and mercaptopropionic acid (MPA){Fig.5 (a)}. The cleavage activity of **1** and **2**were significantly enhanced by these activators and follows the order MPA > H_2O_2>Asc> GSH for **1**, while **2** follows the order MPA >Asc> H_2O_2>GSH.

3.3.3 Effect of radical scavengers on DNA cleavage

In order to investigate the role of reactive oxygen species in the cleavage activity of DNA, comparative DNA cleavage experiments in the presence different common scavengers such as DMSO and Ethyl alcohol (hydroxyl radical scavengers), NaN_3 (singlet oxygen scavenger) and SOD (superoxide oxygen scavenger) were used prior to the addition of **1** and **2** to DNA solution.. As shown in Fig. 5(b) the cleavage activity **1** and **2** was reduced dramatically in the presence of hydroxyl radical scavenger's ethyl alcohol and DMSO Fig. 6(a), indicating that the freely diffusible hydroxyl radical is one of the intermediates involved in the DNA scission process. On the other hand, addition of NaN_3 and SOD (Lanes 2, 3 for **1** and Lanes 6, 7 for **2**, 4 respectively), also do not attenuate the DNA strand scission and even in presence of SOD the cleavage reaction was quite enhanced.These results suggested that hydroxyl radicals, singlet oxygen and superoxide anion radicals are not involved in the DNA cleavage system.Since the complexes **1** and **2**are able to cleave DNA in the absence of any reducing agent, it might be assumed that a discernible hydrolytic path might cleave DNA.

3.3.4 DNA cleavage in presence of recognition elements (groove binding)

DNA recognition elements, minor groove binding agent (DAPI) and major groove binding agent (Methyl Green) [38,39] were used to probe the potential interacting sites of complexes **1** and **2**with pBR322 DNA Fig. 6(b). The cleavage patterns, demonstrated that in presence of methyl green DNA cleavage activity is affected significantly, suggesting that minor groove are involved in the complex–DNA interactions.

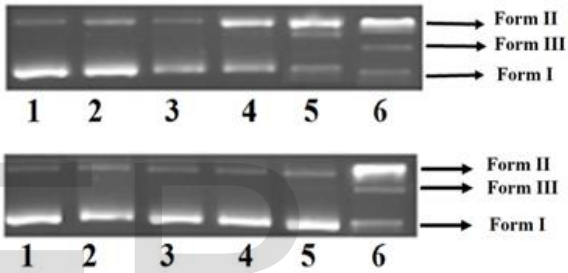

Fig. 5(a). The cleavage patterns of the agarose gel electrophoresis diagram showing cleavage of pBR322 supercoiled DNA (300 ng) by **1** and **2** at 310 K after 45 min of incubation; Lane 1, DNA control; Lane 2, 5 μM of **1** + DNA; Lane 3, 10 μM of **1** + DNA; Lane 4: 20 μM of **2** + DNA; Lane 5: 30 μM of **1** + DNA; Lane 6: 40 μM of **2** + DNA.

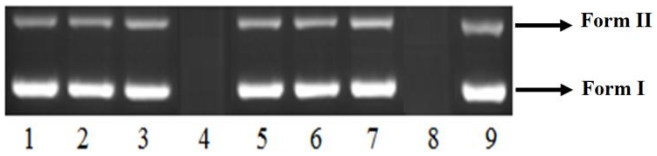

Fig. 5(b). Agarose gel electrophoresis pattern for the cleavage of pBR322 supercoiled DNA (300 ng) by **1** and **2** in presence of different activating agents at 310 K after incubation for 45 min. Lane 1: DNA control; Lane 2: 40 **1** + H_2O_2 (0.4 M) + DNA; Lane 3: 40 μM of **1** + Ascorbic acid (0.4 M) + DNA; Lane 4: 40 μM of **1** + MPA (0.4 M) + DNA; Lane 5: 40 μM of **1** + GSH (0.4 M) + DNA; Lane 6: 40 μM of **2** + H_2O_2 (0.4 M) + DNA; Lane 7: 40 μM of **2** + Ascorbic acid (0.4 M) + DNA; Lane 8: 40 μM of **2** + MPA (0.4 M) + DNA; Lane 9: 40 μM of **2** + GSH (0.4 M) + DNA.

3.4. Molecular docking with DNA

Recently, molecular docking techniques are widely used to visualize experimental structures available for the drug–DNA interactions in rational drug design, as well as in the development of small molecule therapeutics. Targeting the minor groove of DNA through binding to a small molecule has long been considered an important tool in molecular recognition of a specific DNA sequence [40–42]. In order to get more insight into the mode of binding, complexes 1 and 2 were successively docked with DNA duplex of sequence d(CGCGAATTCGCG)$_2$ dodecamer (PDB ID:1BNA), and provide an energetically favorable docked pose that is shown in Fig. 7 (a, b). The results shows that complexes **1** and **2** interacts with DNA *via* an electrostatic mode involving outside edge stacking interactions with the oxygen atom of the phosphate backbone of DNA. In this model, complexes **1** and **2** are snuggly fitted into the curve contour of DNA minor groove in the G–C(~ 13.2 ˚A) ones, and slightly bends the DNA in such a way that a part of the aromatic rings of o–phenylenediamine ligand makes more effective π–π stacking and π–cation interactions between DNA base pairs and lead to van der Waals interaction with the DNA functional groups which define the stability of groove. Moreover, the dipeptide ring of the complexes were arranged in a parallel fashion with respect to the deoxyribosegroove walls of the DNA and was stabilized by hydrogenbonding (2.8–3.8 Å) between the amino group and DC11 residue (3.11˚A), chlorine and DC16 residue (3.27˚A) for complex **1** whereas carbonyl group of peptide shows strong hydrogenbonding with the DC23 residue at a distance of 3.07˚A for complex **2** in the GC region of the minor groove. The resulting relative binding energy of docked metal complexes **1** and **2** with DNA were found to be −260.6 and –218.8 kJ mol^{-1}, respectively. This value is consistent with the high binding constant obtained from spectroscopic titration and groove binding in presence of minor groove binder DAPI and major groove binder MG from DNA cleavage studies.

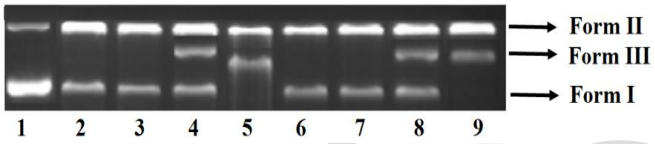

Fig. 6(a). Agarose gel electrophoresis pattern for the cleavage of pBR322 supercoiled DNA (300 ng) by by**1** and **2** in presence of Reactive oxygen species at 310 K after incubation for 45 min. Lane 1: DNA control; Lane 2: 40 μM of **1** + tert–butyl alcohol (0.4 M) + DNA; Lane 3: 40 μM of **1** + DMSO (0.4 M) + DNA; Lane 4: 40 μM of **1** + NaN_3 (0.4 M) + DNA; Lane 5: 40 μM of **1** + SOD (15 units) + DNA; Lane 6: 40 μM of **2** + tert–butyl alcohol (0.4 M) + DNA; Lane 7: 40 μM of **2** + DMSO (0.4 M) + DNA; Lane 8: 40 μM of **2** + NaN_3 (0.4 M) + DNA; Lane 9: 40 μM of **2** + SOD (15 units) + DNA.

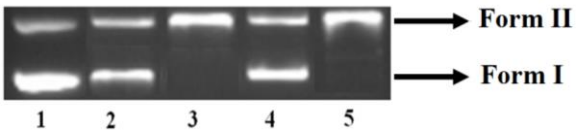

Fig. 6(b). A garose gel electrophoresis pattern for the cleavage of pBR322 supercoiled DNA (300 ng) by by**1** and **2** in presence of DNA minor binding agent DAPI and major binding agent methyl green at 310 K after incubation for 45 min. Lane 1, DNA control; Lane 2, 40 μM of **1** + DNA + DAPI (8 mM); Lane 3, 40 μM of **1** + DNA + methyl green (2.5 mL of a 0.01mg/ml solution); Lane 4, 40 μM of **2** + DNA + DAPI (8 mM); Lane 3, 40 μM of **2** + DNA + methyl green (2.5 mL of a 0.01mg/ml solution).

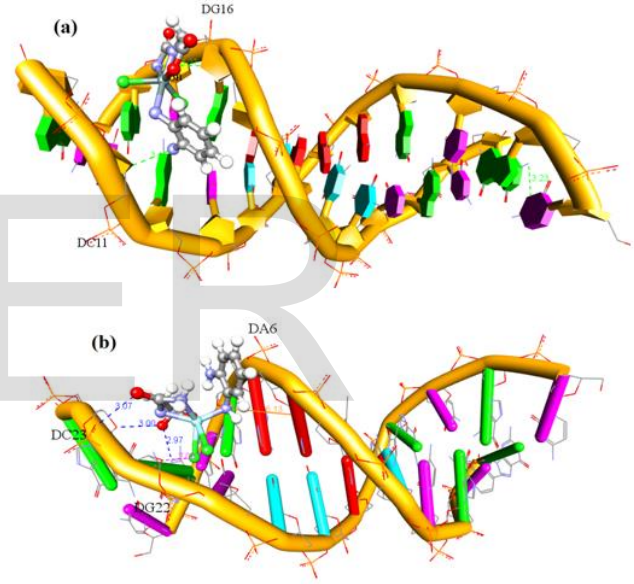

Fig. 7. Molecular docked model of complexes (a) 1 and (b) 2 with DNA dodecamer duplex of sequence d(CGCGAATTCGCG)$_2$ (PDB ID: 1BNA).

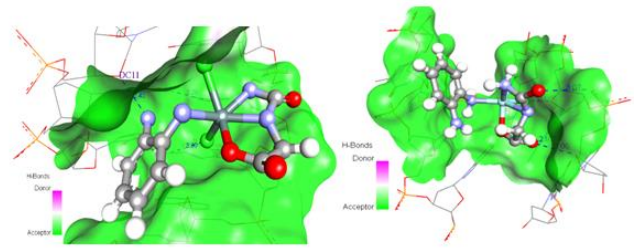

Fig. 8. Molecular docked model of complexes (a) 1 and (b) 2 showing chemically significant hydrogen–bonding with DNA dodecamer duplex of sequence d(CGCGAATTCGCG)$_2$ (PDB ID: 1BNA).

4 Conclusion

We describe herein, the synthesis and characterization of newtin(IV) and zirconium(IV) complexes **1** and **2,** respectively derived from the dipeptide (glygly) and o–phenylenediamine ligand scaffold. The tin(IV) complex **1** shows electronic analogy to zirconium(IV) complex **2** ,therefore their comparative DNA binding propensity was evaluated by employing various biophysical techniques. The spectroscopic binding titrations show that **1** was more avid DNA binding agent as compared to **2**. The cleavage efficiency of **1** and **2** was demonstrated with pBR322 plasmid DNA and it was observed that both the complexes undergo prominent double–strand DNA cleavage in a concentration dependent manner by the hydrolytic pathway. Both complexes are highly efficient nuclease agents due to its ability to perform direct double strand cleavage. Double–strand breaks in DNA duplex are thought to be more significant sources of cell death and genomic instability than single strand breaks, as they are less readily repaired by DNA repair mechanisms.These studies were additionally validated by computational docking technique with target molecules to examine its mode of DNA binding and the studies revealed the electrostatic interaction, in addition to selective binding towards the minor groove of DNA in G/C rich sequences.

Acknowledgments

The authors are highly indebted to the Sophisticated Analytical Instrumentation Facility, Panjab University, Chandigarh, for NMR and ESI–Mass facility; STIC, Cochin for providing elemental analysis. Thanks are also due to Dr. Rizwan H. Khan, Interdisciplinary Biotechnology Unit, AMU, Aligarh for providing the CD facility.

References

[1] (a) Reedijk, J., 1996., Chem. Commun. 801–806;(b)Katja, D. M., Chris, O., 2014. Chem. Rev. 114, 8, 4540–4563.

[2] (a) Sabah, A. A. E., Manal, S., Tianfeng, C., Waddhaah, M. A., 2018. Appl. Organometal. Chem. e4651.; (b) van Rijt, S. H., Sadler, P. J., 2009 Drug Discov. Today 14, 1089–1097.

[3] Crowe, A.J., Fricker (Ed.), in: S.P., 1994. Metal Compounds in Cancer Therapy, Chapman and Hall, London, 147.

[4] Crowe, A. J., 1989. In Metal–Based Antitumour Drugs, 1, M. Gielen (ed.) 103.

[5] Gielen,M., 1995. Met Based Drugs. 2, 99–103.

[6] Vos, D. de, Willem, R., Gielen, M., Wingerden K. E. V., Nooter, K., 1998.Met Based Drugs. 5, 179–188.

[7] Hoti, N., Zhu, D., Song, Z., Wu, Z., Tabassum, S., Wu, M., 2004. J. Pharmacol. Exp. Ther. 311, 427–440.

[8] Chauhan, M., Banerjee, K., Arjmand, F., 2007. Inorg. Chem. 46, 3072–3082.

[9] Mathieu, C., Marc, P., Frédéric, P., Daniel, R. T., Bruno, B., Charles, T., 2012. JBIC J. Biolog. Inorg. Chem. 17, 399–407.

[10]Claussen, C. A., Long, E. C., 1999. Chem. Rev. 99, 2797–2816.

[11] Karidi, K., Garoufis, A., Hadjiliadis, N., Lutz, M., Spek, A. L., Reedijk, J., 2006. Inorg. Chem. 45, 10282−10292.

[12] Sudhamani, C. N., Naik, B., Girija1, H. S., Aravinda, D. T., 2011. International Research Journal of Pure & Applied Chemistry, 1(2); 42–57.

[13] Ryoichi, N., Koshigoe, T., Chikira, M., Long, E. C., 2001. J. Inorg. Biochem. 83, 17–23.

[14] Cardinale, D., Guaitoli, G., Tondi, D., Luciani, R., Henrich, Outi M. H. Salo–Ahen, S., Ferrari, Marverti, S., Guerrieri, G., Ligabue, D., Frassineti, A., Pozzi, C., Manganid, C., Fessas, S., Guerrinif, D., Ponterini, R., Wadeb, G., Costi, R.C., Proc, M.P., 2011. Nat. Acad. Sci. 108, E542–E549.

[15](a)Huber, F., Barbieri, R., 1993. in: B.K. Keppler (Ed.), Metal Complexes in Cancer Chemotherapy, VCH, Weinheim, , pp. 353–363; (b) Arjmand, F., Jamsheera, A., 2011. J. Organomet. Chem. 696, 3572–3579.

[16] Zelder, F. H., Mokhir, A. A., Kramer, R., 2003. Inorg. Chem. 42, 8618−8620.

[17] Arjmand, F., Muddassir, M., Zaidi, Y., Ray, D., 2013. Med. Chem. Commun. 4, 394–405.

[18] Tabassum, S., Al–Asbahy, W. M., Afzal, M., Arjmand, F., Bagchi, V., 2012. Dalton Trans. 41, 4955–4964.

[19] Yang, C. T., Moubaraki, B., Murray, K. S., Vittal, J. J., 2003. Dalton Trans. 5, 880–889.

[20] Manessi–Zoupa, E., Perlepes, S. P., Hondrellis, V., Tsangaris, J. M., 1994. J. Inorg. Biochem. 55, 217–233.

[21] Tabassum, S., Zaki, M., Arjmand, F., Ahmad, I., 2012. J. Photochem. Photobiol. B. 114, 108–118.

[22] Tiliakos, M., Katsoulakou, E., Nastopoulos, V., Terzis, A., Raptopoulou, C., Cordopatis, P., Manessi–Zoupa, E., 2003. J. Inorg. Biochem. 93, 109–118.

[23] Sousa, G.F. de, Deflon, V. M., Gambardella, M. T. P., Francisco, R. H. P., 2006. Inorg. Chem. 45, 4518–4525.

[24] Honga, M., Yin, H., Zhanga, X., Li, C., Yue, C., Cheng, S., 2013. J. Organomet. Chem. 724, 23–31.

[24] Soliman, A. A., 2006. Spectrochim. Acta A. 65 (5); 1180–1185.

[25] Yin, H. D., Wang, Q. B., Xue, S. C., 2004. J. Organmet. Chem. 689, 2480–2485.

[26] Xu, H., Zheng, K., Chen, Y., Li, Y. Z., Lin, L. J., Li, H., Zhang, P.X., Ji, L. N., 2003. Dalton Trans. 2260–2268.

[27] Tan, L. –F., Chao, H., Zhen, K. –C., Fei, J. –J., Wang, F., Zhou, Y. –F., Ji, L. –N., 2007. Polyhedron. 26, 5458–5468.

[28] Pettinari, C., Marchetti, F., Pettinari, R., Martini, D., Drozdov, A., Troyanov, S., 2001.Inorgan. Chim. Acta 325, 103–114.

[29] Wolfe, A., Shimmer, G. H., Meehan, T., 1987. Biochem. 26, 6392–6396.

[30] Dehand, J., Jordanov, J., Keck, F., Mosset, A., Bonnet, J.J., Galy, 1979. J., Inorg. Chem. 18; 1543–1549.

[31] Pettinari, C., Caruso, F., Zaffaroni, N., Villa, R., Marchetti, F., Pettinari, R., Phillips, C., Tanski, J., Rossi, M.J., 2006. Inorg. Biochem. 100, 58–69.

[32] Krishna, P. M., Reddy, K. H., Krishna, P. G., Phillip G. H., 2007. Ind. J. Chem. 46; 904–908.

[33] Blackburn, G. M., Gait, M. J., 1996. Nucleic Acids in chemistry and biology, 2nd Eds, Oxford University Press: New York. 329.

[34] Wilson, W. D., Ratmeyer, L., Zhao, M., Strekowski, L., Boykin, D., 1993. Biochemistry 32 (15); 4098– 4104.

[35] Reinhardt, C. G., Krugh, T. R., 1978. Biochemistry 17, 4845–4854.

[36] Lepecq, J. –B., Paoletti, C., 1967. J. Mol. Biol. 27, 87–106.

[39] Indumathy, R., Radhika, S., Kanthimathi, M., Weyhermuller, T., Nair, B. U., 2007. J. Inorg. Biochem. 101(3); 434–443.

[37] Grover, N., Gupta, N., Singh, P., Thorp, H. H., 1992. Inorg. Chem. 31, 2014–2020.

[38] Banerjee, T., Dubey, P., Mukhopadhyay, R., 2012. Biochimie, 94(2), 494–502.

[39] Barton, J. K., Danishefsky, A. T., Goldberg, J. M., 1984. J. Am. Chem. Soc. 106, 2172–2176.

[40] Trotta, E., Del Grosso, N., Erba, M., Paci, M., 2000. Biochem. 39, 6799–6808.

[41] Wittung, P., Nielsen, P., Norden, B., 1996. J. Am. Chem. Soc. 118, 7049–7054.

[42] De Castro, L. F. P., Zacharias, M., 2002. J. Mol. Recognit. 15, 209–220.